J. Biochem. 123, 33-41 (1998)

Nonadditive Effects of Double Mutations at the Flexible Loops, Glycine-67 and Glycine-121, of *Escherichia coli* Dihydrofolate Reductase on Its Stability and Function

Eiji Ohmae,* Koji Iriyama,† Shigeyuki Ichihara,† and Kunihiko Gekko*,[1]

*Department of Materials Science and Graduate Department of Gene Science, Faculty of Science, Hiroshima University, Kagamiyama, Higashi-Hiroshima 739; and †Department of Applied Biological Science, Faculty of Agriculture, Nagoya University, Chikusa-ku, Nagoya, Aichi 464-01

Received for publication, May 30, 1997

The structure, stability, and enzymatic function of dihydrofolate reductase (DHFR) from *Escherichia coli* are influenced by point mutations at sites 67 and 121 in two flexible loops [Gekko *et al.* (1994) *J. Biochem.* 116, 34-41; Ohmae *et al.* (1996) *J. Biochem.* 119, 703-710]. In the present study, eight double mutants at sites 67 and 121 (G67V/G121S, G67V/G121A, G67V/G121C, G67V/G121D, G67V/G121V, G67V/G121H, G67V/G121L, and G67V/G121Y) were constructed in order to identify interactions between the two sites of DHFR. The far-ultraviolet circular dichroism spectra of double mutants were clearly different from those of the respective single mutants, with significant changes being observed for three mutants, G67V/G121A, G67V/G121L, and G67V/G121S. The Gibbs free energy change of urea unfolding of double mutants could not be expressed by the sum of those of the respective single mutants except for G67V/G121H. The steady-state kinetic experiments showed that the effect of double mutations manifests itself not in K_m but in k_{cat}, and the transition-state stabilization energy for G67V/G121A, G67V/G121C, and G67V/G121L is not equal to the sum of those for the single mutants. These results indicate that the additivity rule essentially does not hold for these double mutants, and that long-range interactions occur between sites 67 and 121, even though they are separated by 27.7 Å. This is evidence that the flexible loops play important roles in the stability and function of this enzyme through structural perturbations, in which a small alteration in local atomic packing due to amino acid substitution is cooperatively magnified over almost the whole molecule.

Key words: dihydrofolate reductase, double mutants, flexible loops, long-range interactions, stability and function.

Dihydrofolate reductase (DHFR) [EC 1.5.1.3] from *Escherichia coli* is an excellent example for studying the structure-flexibility-function relationship of enzymes. As revealed by X-ray crystallographic studies (*1-3*), DHFR has several flexible loops in the molecule, residues 9-24, 64-72, 117-131, and 142-149 (Fig. 1). Recent NMR study showed that sites 67 and 121 in these loops have the extremely large order parameters (*4*). This means that these sites fluctuate extensively in solution, although their functions are unknown. In the previous papers (*5, 6*), we found that site-directed mutagenesis at glycine-121 in a flexible loop (residues 117-131) significantly influences the stability and enzyme function, although the α-carbon at this site is 19.1 Å distant from the catalytic residue Asp27. Recently, mutation at glycine-67 in another flexible loop (residues 64-72) was also found to affect the stability and the hydride transfer reaction, although this position, being 28.7 Å distant from Asp27, should not directly participate in the enzyme reaction, like site 121 (*7*). These results suggest that the flexible loops play important roles in the stability and function of this enzyme, and that the effect of the mutations extends over a long distance *via* modified flexibility of the structure.

To address this issue, double mutants may be useful because the measured energetic data can be compared with those of the corresponding single mutations. In many cases, the sum of the free energy changes derived from single mutations is nearly equal to the free energy change measured in the double mutant (*8-13*). However, there are a number of exceptions where such additivity breaks down, depending on the proteins and mutation sites. Nonadditive effects mean that the mutated residues interact with each other by direct contact or long-range forces such as electrostatic interactions and structural perturbations (*14-17*). Despite many single mutation studies, few reports have appeared on double mutation of DHFR. Perry *et al.* (*18*) reported that L28R/E139Q receives the additive effects from each mutation at sites 28 and 139 in the kinetic refolding and the equilibrium unfolding, but L28R/E139L does not. Texter *et al.* (*19*) reported that the intramolecular hydrogen bonds between Arg44 and Pro66 accelerate

[1] To whom correspondence should be addressed.

Abbreviations: ASA, accessible surface area; CD, circular dichroism; DHFR, dihydrofolate reductase; H_2F, dihydrofolate.

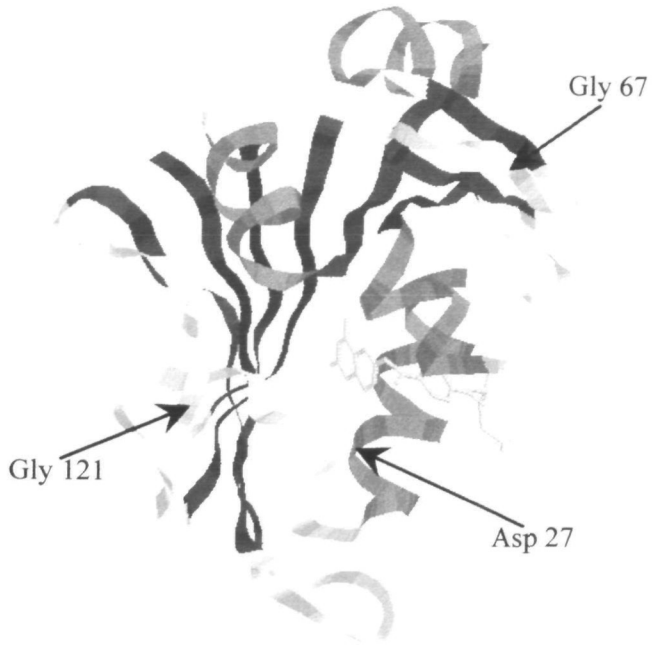

Fig. 1. **Crystal structure of a DHFR-methotrexate binary complex.** Taken from Bolin *et al.* (*1*). α-Helices and β-sheets are indicated by dark gray and black, respectively. The mutation sites, Gly67 and Gly121, and a catalytic residue, Asp27, are indicated by arrows. The α-carbons of Gly67 and Gly121 are separated by 27.7 Å. The distances of the α-carbons of Gly67 and Gly121 from Asp27 are 28.7 and 19.1 Å, respectively.

the *cis-trans* isomerization of the Glu65-Pro66 peptide bond and play a crucial role in the rate-limiting steps of the folding reaction. Dion *et al.* (*20*) found that in D27S/F153S and D27S/I155N, the second mutations at sites 153 and 155 partially restored the dihydrofolate reduction activity which was depressed by the mutation from aspartic acid to serine at active site 27. These results imply that the effect of double mutations of DHFR might be nonadditive, depending on the mutation sites, through their close or indirect interactions. Identifying how far the effect of mutations at a given site can reach should give new insight into the structural dynamics and folding mechanism of this enzyme.

From these viewpoints, in the present study, we have constructed eight double mutants at sites 67 and 121 in two flexible loops of DHFR (G67V/G121A, G67V/G121C, G67V/G121D, G67V/G121H, G67V/G121L, G67V/G121S, G67V/G121V, and G67V/G121Y). Although the distance between the α-carbons at both sites is 27.7 Å (Fig. 1), surprisingly, nonadditivity was observed in the circular dichroism (CD) spectra, free energy of urea unfolding, and steady-state kinetic parameters. These results will be discussed in terms of the characteristic long-range interactions between the two sites, in relation to the role of the flexible loops.

MATERIALS AND METHODS

Plasmid and Mutant Constructions—All mutant plasmids were constructed from plasmid pKGY26 (5.3 kb), an expression vector coding a G67V mutant DHFR (*7*). Since all mutant plasmids constructed from pTP64-1 (*21*) coding the wild-type DHFR have three *Pvu*I digestive sites, one being located between the two mutation sites (sites 67 and 121), a DNA fragment coding the latter half of the G67V gene was recombined with a corresponding fragment of the site 121 mutant DHFRs by the following method. In the first step, plasmid pKGY26 was partially digested by *Pvu*I. The resulting 4-kb fragment, which has the former half of the DHFR gene, was separated by agarose gel electrophoresis and recovered by use of a GENECLEAN® II kit (Bio 101). Then the purified fragment was self-ligated by use of a DNA ligation kit (Takara) and used for transformation of an *E. coli* HB101 strain. Transformants were selected on a LB-plate containing 50 μg/ml ampicillin and 20 μg/ml trimethoprim. In the second step, the purified plasmid from the transformant was partially digested by *Pvu*I and ligated with a 1.3-kb fragment coding the mutant DHFRs at site 121, which has the latter half of the DHFR gene. The ligated plasmid was introduced into *E. coli* JM109 strain and transformants were selected by their ampicillin- and trimethoprim-resistant phenotypes on an M9-plate containing 0.2% glucose, 30 μg/ml ampicillin, and 5 μg/ml trimethoprim. Recombinant *fol* genes were checked by DNA sequencing (*22*) with an Applied Biosystems Model 373A DNA sequencer to avoid unexpected mutation.

Protein Purification—Mutant DHFRs were expressed in *E. coli* strain D3-157, which lacks the chromosomal *fol* gene (*23*). The mutant proteins were purified by the same method as the wild-type DHFR (*7*). Protein concentration was determined spectrophotometrically using a molar extinction coefficient of 31,100 $M^{-1}\cdot cm^{-1}$ at 280 nm (*24*). This value was corrected for the absorption of an introduced tyrosine residue in G67V/G121Y to be 32,300 $M^{-1}\cdot cm^{-1}$. Such correction was not done for the histidine and cysteine mutants because their absorption at this wavelength is negligibly small.

Circular Dichroism Spectra—Far-ultraviolet circular dichroism (CD) spectra were measured with a Jasco J-720W spectropolarimeter at 15°C. The buffer used was 10 mM potassium phosphate (pH 7.0) containing 0.1 mM dithiothreitol and 0.1 mM EDTA. Protein concentrations were kept at about 20 μM. When the spectra in 6 M urea solution were measured, samples were preincubated for 10 h to allow complete unfolding.

Equilibrium Unfolding—Equilibrium unfolding of double mutant DHFRs with urea (ultrapure product from Schwarz/Mann) was monitored by means of CD measurements at 222 nm and 15°C with a Jasco J-40A spectropolarimeter as described previously (*5*). The solvent used was 10 mM potassium phosphate (pH 7.0) containing 0.1 mM EDTA and 1.4 mM 2-mercaptoethanol. The protein concentration was kept at about 10 μM. All samples were fully equilibrated at each denaturant concentration before the CD spectra were measured.

The observed molar ellipticity data, $[\theta]$ (38 points), were directly fitted to the two-state unfolding model, native (N)$\rightleftharpoons$unfolded (U), by means of a nonlinear least-squares regression analysis with a SALS program (*25*), as follows

$$[\theta]=\{[\theta]_N+[\theta]_U\exp(-\Delta G_u/RT)\}/\{1+\exp(-\Delta G_u/RT)\} \quad (1)$$

where ΔG_u is the Gibbs free energy change of unfolding, R the gas constant, T the absolute temperature, $[\theta]_N$ and

$[\theta]_U$ the molar ellipticities of the native and unfolded forms, respectively. $[\theta]_N$ and $[\theta]_U$ at a given urea concentration were estimated by assuming the same linear dependence of ellipticity in the transition region as in the pure native (pre-transition region) and unfolded states (post-transition region). The free energy of unfolding, ΔG_u in Eq. 1, was calculated by assuming its linear dependence on the urea concentration (*26*)

$$\Delta G_u = \Delta G_u^\circ + m[\text{urea}] \quad (2)$$

where ΔG_u° is the free energy change of unfolding in the absence of denaturant, and the slope, m, is a parameter reflecting the cooperativity of the transition. The urea concentration at the midpoint of the transition ($\Delta G_u = 0$) was defined as C_m.

Steady-State Kinetics—Steady-state kinetics of the enzyme reaction were studied by using a Jasco UVIDEC-610C spectrophotometer at 25°C. Dihydrofolate (H_2F) and NADPH concentrations were determined with molar extinction coefficients of 28,000 $M^{-1}\cdot cm^{-1}$ at 282 nm and 6,200 $M^{-1}\cdot cm^{-1}$ at 339 nm, respectively. The enzyme concentrations were determined by a methotrexate titration method (*27*) to eliminate the effects of denatured species which may be produced during storage. The enzyme solution was preincubated with NADPH for 10 min to eliminate the hysteresis effect (*28*). Final concentrations of the reaction mixtures were 100 mM imidazole hydrochloride (pH 7.0), 12 mM 2-mercaptoethanol, 60 μM NADPH, 0.5-20 μM H_2F, and 1-20 nM enzyme. The initial velocities (v) of enzyme reaction were calculated from the time course of absorbance at 340 nm using a differential molar extinction coefficient of 11,800 $M^{-1}\cdot cm^{-1}$ (*29*). The Michaelis constant (K_m) and the rate constant of catalysis (k_{cat}) in the following equation were determined by the nonlinear least-squares method with a SALS program

$$v = (k_{cat}[E][S])/(K_m + [S]) \quad (3)$$

where [E] is the enzyme concentration and [S] the initial substrate concentration.

RESULTS

Circular Dichroism Spectra—Figure 2 shows the typical far-ultraviolet CD spectra of the wild-type and mutant DHFRs at pH 7.0 and 15°C. Similar spectra were also observed for other mutant DHFRs, indicating that all mutants constructed have the native conformation under these conditions (data not shown). As we reported previously (*5-7*), however, the CD spectrum of native DHFR is influenced by the single amino acid substitution. G67V has a negative peak of −7,400 deg·cm²·dmol⁻¹ at 222 nm and a positive peak of 9,500 deg·cm²·dmol⁻¹ at 195 nm (Fig. 2A), which are obviously different from the peak ellipticities of the wild-type DHFR, −8,500 deg·cm²·dmol⁻¹ at 219 nm and 11,200 deg·cm²·dmol⁻¹ at 196 nm. The large negative ellipticity around 230 nm observed for G67V might be ascribed to disruption of an exciton pair of tryptophans 47 and 74 (*7, 30*). Five double mutant DHFRs, G67V/G121C, G67V/G121D, G67V/G121H, G67V/G121V, and G67V/G121Y (data not shown), showed similar spectra to G67V, although the respective single mutants at site 121 have characteristically different spectra (*6*). On the other hand, three double mutant DHFRs, G67V/G121A, G67V/G121S, and G67V/G121L, showed considerably different spectra from those of G67V and the respective single mutants. As shown in Fig. 2A, G67V/G121A has a negative peak of −8,300 deg·cm²·dmol⁻¹ at 222 nm and a positive peak of 11,100 deg·cm²·dmol⁻¹ at 195 nm. These values are close to those of G121A, but the ellipticity around 230 nm is much smaller than those of G121A and G67V. As shown in Fig. 2B, G67V/G121S showed a very small negative ellipticity of −6,800 deg·cm²·dmol⁻¹ at 220 nm and a positive peak of 9,300 deg·cm²·dmol⁻¹ at 195 nm, different from the spectra of G67V and G121S (*7*). These results indicate that the effects of double mutation on the CD spectra or native structure cannot be expressed as the sum of the contributions of the respective single mutants.

Despite the CD changes in the native state, all mutant and wild-type DHFRs showed the same spectra in 6 M urea (Fig. 2A). Thus, the conformation of unfolded DHFR may be essentially identical in all mutants.

Equilibrium Unfolding—Figure 3 shows typical plots of the apparent native fraction of the wild-type and mutant DHFRs as a function of the urea concentration at 15°C and pH 7.0. Similar transition curves were also observed for other mutant DHFRs (data not shown). The unfolding of the

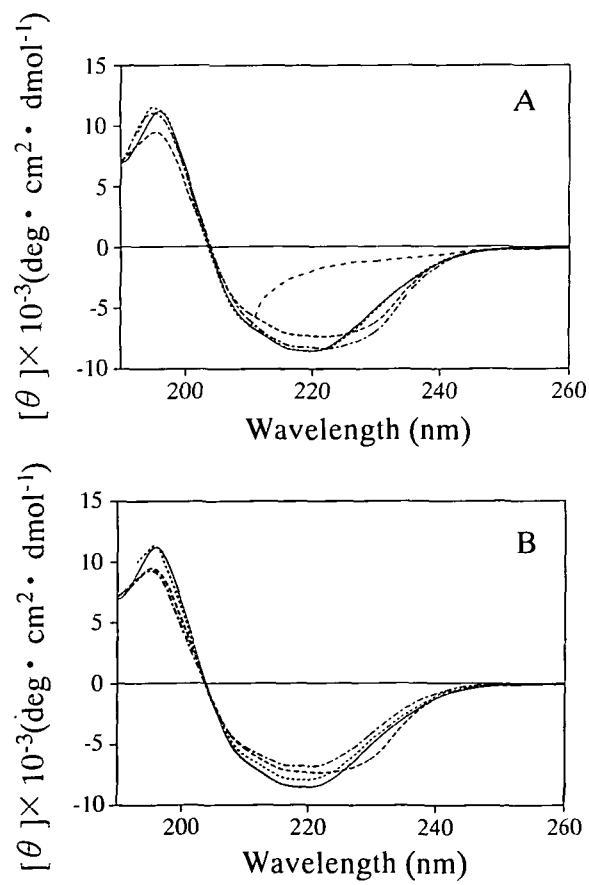

Fig. 2. **Far-ultraviolet circular dichroism spectra of the wild-type and typical mutant DHFRs at 15°C.** The solvent used was 10 mM potassium phosphate (pH 7.0) containing 0.1 mM EDTA and 0.1 mM dithiothreitol. (A): (—) Wild-type DHFR; (·····) G67V; (·····) G121A; (-·-·-) G67V/G121A; (-·-·) wild-type DHFR in a 6 M urea solution. (B): (—) Wild-type DHFR; (·····) G67V; (·····) G121S; (-·-·-) G67V/G121S.

double mutant DHFRs essentially followed the two-state transition model, as found for the wild-type and single mutant DHFRs (*5-7, 31-33*). As shown in Fig. 3A, the double mutant G67V/G121A showed the transition at much higher urea concentration than did the respective single mutants, G67V and G121A. On the other hand, the transition of G67V/G121D occurred at lower urea concentration than those of the corresponding single mutants, G67V and G121D (Fig. 3B). These results suggest that the effects of mutation of site 121 on the structural stability of DHFR depends on the residues at site 67.

The free energy change of unfolding in the absence of urea, ΔG°_{u}, the slope, m, and the denaturant concentration at $\Delta G_u = 0$, C_m, which were calculated using Eqs. 1 and 2, are listed in Table I with the results for the wild-type and single mutant DHFRs. As shown in this table, the ΔG°_{u} values varied in the range of 4.77 kcal/mol (G67V/G121D) to 7.08 kcal/mol (G67V/G121Y). The stability of the double mutants decreased in the order of the residues at site 121, Tyr > Ala > Ser > Val ≧ Gly > Leu ≧ His > Cys ≧ Asp. This order was not consistent with that for the single mutants at site 121 (*6*). Interestingly, the double mutant G67V/G121Y was more stable than the wild-type DHFR, although the corresponding single mutants, G67V and G121Y, were less stable. These results clearly demonstrate that there is no additivity in the mutation effects at sites 67 and 121. Such nonadditivity in the stability was also observed for all other double mutants except for G67V/G121H (see "DISCUSSION").

As shown in Table I, the m value was also affected by the double mutations as well as the single mutations at sites 67 and 121. The m values of double mutants were in the range of −1.77 kcal/mol·M (G67V/G121C) to −2.19 kcal/mol·M (G67V/G121Y), which are comparable or slightly less negative as compared with those of single mutants at site 121, −1.92 kcal/mol·M (G121V) to −2.32 kcal/mol·M (G121D). A noticeable difference was found in the C_m

TABLE I. **Thermodynamic parameters for urea denaturation of the wild-type and mutant DHFRs at 15°C.**[a]

DHFR	ΔG°_{u} (kcal/mol)	m (kcal/mol·M)	C_m(M)
Wild-type[b]	6.08±0.18	−1.96±0.06	3.11
G67V[c]	5.14±0.17	−1.78±0.05	2.89
G67V/G121S	5.86±0.14 (6.09)	−2.15±0.05 (−2.01)	2.72 (3.03)
G67V/G121A	6.73±0.14 (6.58)	−2.00±0.04 (−2.30)	3.36 (2.86)
G67V/G121C	4.78±0.13 (6.17)	−1.77±0.04 (−2.16)	2.69 (2.86)
G67V/G121D	4.77±0.13 (6.27)	−1.91±0.05 (−2.32)	2.50 (2.70)
G67V/G121V	5.15±0.10 (5.09)	−2.05±0.04 (−1.92)	2.51 (2.65)
G67V/G121H	5.05±0.13 (5.97)	−2.01±0.05 (−2.26)	2.51 (2.64)
G67V/G121L	5.07±0.14 (5.45)	−1.85±0.05 (−1.96)	2.73 (2.78)
G67V/G121Y	7.08±0.17 (5.88)	−2.19±0.06 (−2.16)	3.24 (2.72)

[a]The solvent used was 10 mM potassium phosphate (pH 7.0) containing 0.1 mM EDTA and 1.4 mM 2-mercaptoethanol. The parameters ΔG°_{u}, m, and C_m were calculated by assuming a linear relationship between ΔG_u and the urea concentration (Eq. 2). The values in parentheses are for the corresponding single mutants at site 121 (*6*). [b]Gekko *et al.* (*6*). [c]Ohmae *et al.* (*7*).

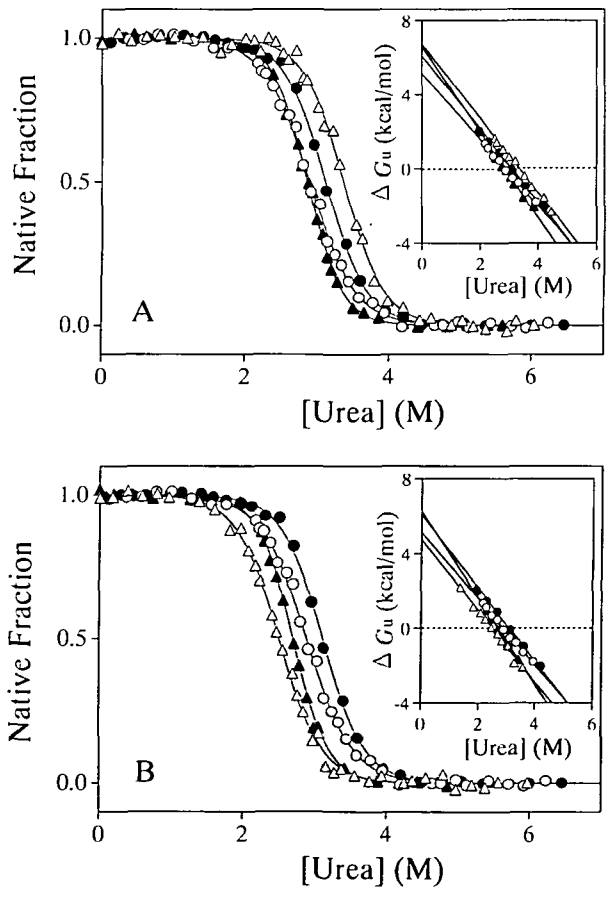

Fig. 3. **Apparent native fraction of the wild-type and typical mutant DHFRs as a function of the urea concentration at 15°C.** The native fraction was monitored by CD at 222 nm. The solvent used was 10 mM potassium phosphate (pH 7.0) containing 0.1 mM EDTA and 1.4 mM 2-mercaptoethanol. (A): (●) Wild-type DHFR; (□) G67V; (▲) G121A; (△) G67V/G121A. (B): (●) Wild-type DHFR; (□) G67V; (▲) G121D; (△) G67V/G121D. Solid lines represent the theoretical fits to a two-state transition model with the parameter values shown in Table I. (Inset): Dependence of the apparent free energy change of unfolding (ΔG_u) on the urea concentration.

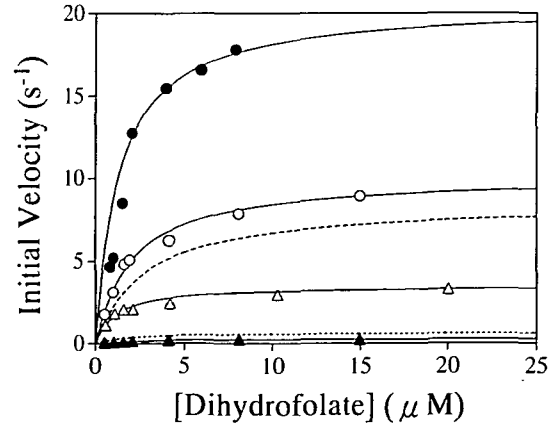

Fig. 4. **Initial velocity of the enzymatic reaction of the wild-type, G67V, and two double mutant DHFRs as a function of the dihydrofolate concentration at 25°C.** The solvent used was 100 mM imidazole hydrochloride (pH 7.0) containing 12 mM 2-mercaptoethanol, 60 μM NADPH, and 0.5-20 μM dihydrofolate. The concentrations of enzymes were 0.5-1.5 nM. (●) Wild-type DHFR; (□) G67V; (▲) G67V/G121D; (△) G67V/G121A. Solid lines represent the theoretical fits to Eq. 3 with the parameter values shown in Table II. A broken line and a dotted line indicate the results for G121A and G121D DHFRs, respectively (*6*).

TABLE II. **Steady-state kinetic parameters for enzyme reaction of the wild-type and mutant DHFRs at 25°C.**[a]

DHFR	K_m (μM)	k_{cat} (s^{-1})	k_{cat}/K_m ($s^{-1}\cdot\mu M^{-1}$)
Wild-type[b]	1.2	20.9	17.4
G67V	2.0±0.1	10.1±0.2	5.1
G67V/G121S	2.1±0.6 (1.8)	1.1±0.1 (5.2)	0.52 (2.9)
G67V/G121A	1.1±0.3 (2.7)	3.5±0.2 (8.5)	3.2 (3.1)
G67V/G121C	2.0±0.5 (1.5)	1.5±0.1 (8.4)	0.75 (5.6)
G67V/G121D	2.4±1.0 (1.6)	0.3±0.1 (0.67)	0.13 (0.42)
G67V/G121V	3.3±0.7 (1.4)	0.7±0.1 (0.94)	0.21 (0.67)
G67V/G121H	1.4±0.7 (2.2)	1.6±0.3 (4.8)	1.1 (2.2)
G67V/G121L	2.0±0.9 (2.3)	2.0±0.3 (0.94)	1.0 (0.41)
G67V/G121Y	2.6±0.8 (2.5)	1.0±0.1 (4.4)	0.38 (1.8)

[a]The solvent used was 100 mM imidazole hydrochloride (pH 7.0) containing 12 mM 2-mercaptoethanol. The values in parentheses are for the corresponding single mutants at site 121 (*6*). [b]Gekko *et al.* (*6*).

values: the C_m values of G67V/G121A and G67V/G121Y (3.36 and 3.24 M, respectively) were larger than that for the wild-type DHFR (3.11 M), although all the single mutant DHFRs at sites 67 and 121 had smaller values.

Steady-State Kinetics—Figure 4 shows typical plots of the initial velocity of the enzyme reaction as a function of the substrate (H_2F) concentration. Similar hyperbolic curves were also observed for other mutant DHFRs. The Michaelis constant, K_m, and the rate constant of catalysis, k_{cat}, were calculated using Eq. 3 and listed in Table II with the results for the wild-type and G67V DHFRs. The K_m values of the double mutants varied in the range of 1.1 μM (G67V/G121A) to 3.3 μM (G67V/G121V), which were not significantly different from that of the wild-type DHFR, 1.2 μM. This was also the case for the single mutants at sites 67 and 121 as previously reported (*6, 7*). These results suggest that the double mutation, like the single mutation at the two sites, does not essentially affect the affinity with the substrate, although G67V/G121V and G67V/G121A may have some cooperative effect as compared with the corresponding single mutants.

On the other hand, the k_{cat} values of the double mutant DHFRs decreased to one-sixth (G67V/G121A) to one-seventieth (G67V/G121D) of that of the wild-type DHFR. These large decreases in k_{cat} of double mutants seem to be dominantly caused by the residues at site 121, because the single mutation at site 121 also remarkably reduced k_{cat}, while the single mutation at site 67 did so only slightly. The larger k_{cat} value of G67V/G121L relative to G121L suggests that the mutations at site 67 could also influence the effect of mutation at site 121 on the kinetics processes.

DISCUSSION

As shown in this study, double mutations at sites 67 and 121 brought about considerable changes in the native structure, stability, and enzyme function of DHFR. These results give useful information on the role of these sites located in flexible loops far from the active site. A matter of concern is how the effects of double mutations can be explained in terms of the contributions of the respective single mutations at two sites. This problem will be discussed below with the free energy diagram for the mutation cycle.

Structure of Mutant DHFRs—As shown in Fig. 2, the CD spectrum of native DHFR was obviously affected by the double mutations at sites 67 and 121 as well as the single mutations at two sites (*5-7*). A characteristic change appears in the ellipticities around 230 nm: they are enhanced for six double mutants, G67V/G121A, G67V/G121C, G67V/G121D, G67V/G121H, G67V/G121V, and G67V/G121Y, but depressed for two double mutants, G67V/G121L and G67V/G121S. More interestingly, the CD spectra of these double mutants can not be expressed as the sum of the respective single mutant CD spectra. These results imply that the mutation at site 121 influences the surroundings of site 67. The most probable explanation for such large CD changes emerges from consideration of the perturbation of the tryptophan exciton pair between Trp47 and Trp74 (*30*): the enhanced ellipticity around 230 nm may be attributed to the disruption of this exciton pair. It is probable that the amino acid substitution or local space modification at site 67 causes perturbation of the exciton pair and influences the peptide CD, because the distance between the nearest atoms of Gly67 and Trp74 is only 3.41 Å (*1*).

Another possible origin of the observed CD changes may involve multiple conformers of this protein. Jennings *et al.* (*34*) found, by the kinetic refolding experiment, that four native or native-like conformers exist in the wild-type DHFR, and Iwakura *et al.* (*35*) showed that they reduce to two conformers by an amino acid substitution at site 85. If the mutations at sites 67 and 121 could reduce one or more conformers, the perturbation of the peptide CD may be induced through movement of the secondary structure and/or aromatic side chains including Trp74 and Trp47. In either case, a detailed understanding of the structural changes must await X-ray or NMR analyses of the mutant enzymes, which are in progress in our laboratory.

Nonadditive Effects on Protein Stability—The urea unfolding profiles of all double mutants examined in the present study sufficiently agreed with the two-state transition model, like those of the wild-type (*31*) and single mutant DHFRs (*5-7, 32, 33*). This means that the local structures around the sites 67 and 121 are broken down cooperatively in the urea unfolding process. However, the effects on the protein stability of mutations at sites 67 and 121 are not necessarily additive. For example, the ΔG°_u value of G67V/G121Y is much larger than that of the wild-type DHFR, although G67V and G121Y have the smaller values. On the other hand, G67V/G121C and G67V/G121D have very small ΔG°_u values, although G121C and G121D have larger values than the wild-type DHFR. G67V/G121A has a larger ΔG°_u value than G121A by overcoming the destabilizing effect of G67V. These results indicate that the mutations at sites 67 and 121 do not independently contribute to the protein stability and that interactions occur between the two sites.

The effects of double mutation on the stability can be quantitatively analyzed by the following free energy diagram (Scheme 1), where N and U are the native and unfolded states, respectively; ΔG^N_{mut} and ΔG^U_{mut} the free energy changes of mutation at the native and unfolded states, respectively; and X the amino acid residues introduced at site 121. According to this diagram, the change in the free energy of unfolding due to mutations at site 121, $\Delta\Delta G^\circ_{G121-X}$, can be expressed as follows when site 67 is glycine (wild) or valine,

$$\Delta\Delta G^\circ_{G67,G121-X} = \Delta G^\circ_{u,G121X} - \Delta G^\circ_{u,wild} \quad (4)$$

$$\Delta\Delta G^{\circ}_{V67,G121\to X} = \Delta G^{\circ}_{u,G67V/G121X} - \Delta G^{\circ}_{u,G67V} \quad (5)$$

If the mutation effect at site 121 is independent of site 67, *i.e.*, the contributions of site 67 and 121 are additive, $\Delta\Delta G^{\circ}_{G67,G121\to X}$ should be identical with $\Delta\Delta G^{\circ}_{V67,G121\to X}$. Thus the difference between Eqs. 4 and 5, $\Delta\Delta\Delta G^{\circ}_{u}$, can be regarded as a measure of nonadditivity or the interaction between the two sites.

$$\Delta\Delta\Delta G^{\circ}_{u} = \Delta\Delta G^{\circ}_{V67,G121\to X} - \Delta\Delta G^{\circ}_{G67,G121\to X}$$
$$= (\Delta G^{\circ}_{u,G67V/G121X} - \Delta G^{\circ}_{u,G67V}) - (\Delta G^{\circ}_{u,G121X} - \Delta G^{\circ}_{u,wild}) \quad (6)$$

The calculated values of $\Delta\Delta G^{\circ}_{G67,G121\to X}$, $\Delta\Delta G^{\circ}_{V67,G121\to X}$, and $\Delta\Delta\Delta G^{\circ}_{u}$ are listed in Table III with the molecular parameters of the amino acid side chains introduced into site 121. It is seen that the $\Delta\Delta\Delta G^{\circ}_{u}$ value is not zero except for the histidine mutant within the estimation errors for calculation. This result clearly confirms the existence of the long-range interaction between the two mutation sites. From crystallographic studies of the wild-type DHFR, the distance between the α-carbons at sites 67 and 121 is 27.4 and 27.7 Å in the apoenzyme and the methotrexate binary complex, respectively (*1, 3*). The long-range interaction is thus expected to extend beyond 27 Å, probably over the whole molecule. Recently, Green and Shortle also reported that nonadditivity is generally observed in 71 double mutants of staphylococcal nuclease and the long-range interaction can extend out 20 Å or more (*16*).

A matter of concern is whether such a nonadditivity is attributed to the modification of native or unfolded state. Green and Shortle proposed the importance of the unfolded structure for the nonadditive stability of staphylococcal nuclease, from the correlation between the $\Delta\Delta\Delta G^{\circ}_{u}$ value and the *m*-value change, $\Delta\Delta m$, based on assumption that the changes in *m*-value are manifestations of changes in the solvation of the unfolded state. Such a correlation between $\Delta\Delta\Delta G^{\circ}_{u}$ and $\Delta\Delta m[=\Delta m_{G67V/G121X} - (\Delta m_{G67V} + \Delta m_{G121X})]$, was also found for our double mutants except for G67V/G121A and G67V/G121Y (correlation coefficient, 0.95) (Table III), suggesting that the nonadditivity in cooperativity of transition causes the nonadditivity in the stability. However, this does not necessarily mean that the nonadditive stability is only due to the unfolded state, because the CD spectra clearly indicate the modification of the native structure (Fig. 2). The nonadditivity of enzyme function, as mentioned below, also supports the importance of the native state. To examine this, statistical analyses of the relationship between $\Delta\Delta\Delta G^{\circ}_{u}$ and some molecular parameters of introduced amino acids may be helpful. Figure 5 shows the plots of the $\Delta\Delta\Delta G^{\circ}_{u}$ values as a function of the hydrophobicity (Δg°_{tr}), volume, and accessible surface area (ASA) of the side chains at site 121. There appears to be some correlation between $\Delta\Delta\Delta G^{\circ}_{u}$ and these parameters, although the correlation coefficients are not high (0.643, 0.441, and 0.353, for Δg°_{tr}, volume, and ASA, respectively). Similar correlations were also found for the single mutants at site121, and we considered that the main effect of a single mutation at site 121 would be modification of the flexibility of the loop due to overcrowding of the bulky side chains, overcoming the enhancement of the hydrophobic interaction (*6*). This would be essentially established for the double mutants, although the local structure around site 121 might be modified by changing site 67 from glycine to valine. These findings are evidence that the origin of nonadditivity lies mainly in the native state. One conceivable source of this nonadditivity is a stepwise atomic rearrangement in the native structure. Such rearrangement would probably extend over the whole molecule, because we recently found that the nonadditivity also holds for some double mutants at sites 121 and 145, which are separated by 25.9 Å (Ohmae *et al.*, to be published).

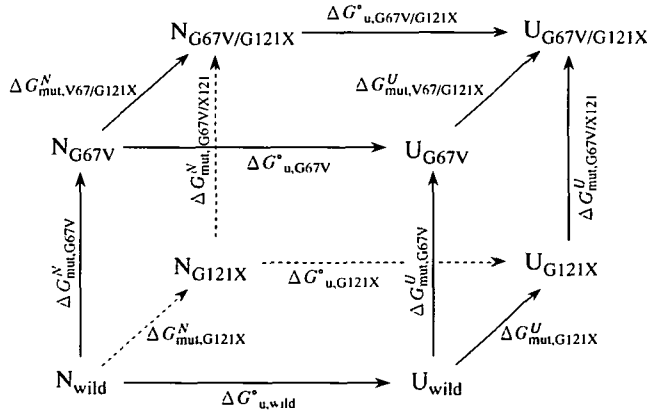

Scheme 1

Nonadditive Effects on Enzyme Function—As shown in Table II, double mutations at sites 67 and 121, as well as single mutations at the respective sites, bring about no significant change in K_m but a large decrease in k_{cat}. The almost constant K_m values suggest that the affinity of substrate to holoenzyme is not substantially modified by these double mutations, as expected by the strong affinity of all the mutants to methotrexate-agarose resin. However,

TABLE III. $\Delta\Delta G^{\circ}_{G121\to X}$, $\Delta\Delta\Delta G^{\circ}_{u}$, and $\Delta\Delta m$ values calculated from the thermodynamic parameters in Table I.

Residue at site 121	Δg°_{tr}[a] (kcal/mol)	Volume[b] (ml/mol)	ASA[c] (Å²)	$\Delta\Delta G^{\circ}_{G121\to X}$ (kcal/mol)[d] Glycine-67	Valine-67	$\Delta\Delta\Delta G^{\circ}_{u}$[e] (kcal/mol)	$\Delta\Delta m$[f] (kcal/mol·M)
Ser	−0.3	51.9	80	0.01±0.24	0.72±0.22	0.71±0.33	−0.32±0.11
Ala	0.5	52.0	67	0.50±0.25	1.59±0.22	1.09±0.32	0.12±0.11
Cys	1.0	65.0	104	0.09±0.28	−0.36±0.21	−0.45±0.35	0.21±0.11
Asp	−2.5	65.4	106	0.19±0.20	−0.37±0.21	−0.56±0.29	0.23±0.10
Val	1.5	82.4	117	−0.99±0.27	0.01±0.20	1.00±0.34	−0.31±0.12
His	0.5	90.3	151	−0.11±0.29	−0.09±0.21	0.02±0.36	0.07±0.13
Leu	1.8	99.2	137	−0.63±0.25	−0.07±0.22	0.56±0.33	−0.07±0.11
Tyr	2.3	114.7	187	−0.20±0.25	1.94±0.24	2.14±0.35	−0.21±0.12

[a]The transfer free energy change of amino acid side chains from organic solvent to water (*42*). [b]The molar volume of amino acid side chains (*43*). [c]The accessible surface area of amino acid side chains (*44*). [d]The $\Delta\Delta G^{\circ}_{G121\to X}$ values were calculated with Eqs. 4 and 5. [e]The $\Delta\Delta\Delta G^{\circ}_{u}$ values were calculated with Eq. 6. [f]$\Delta\Delta m = \Delta m_{G67V/G121X} - (\Delta m_{G67V} + \Delta m_{G121X})$ (see "DISCUSSION").

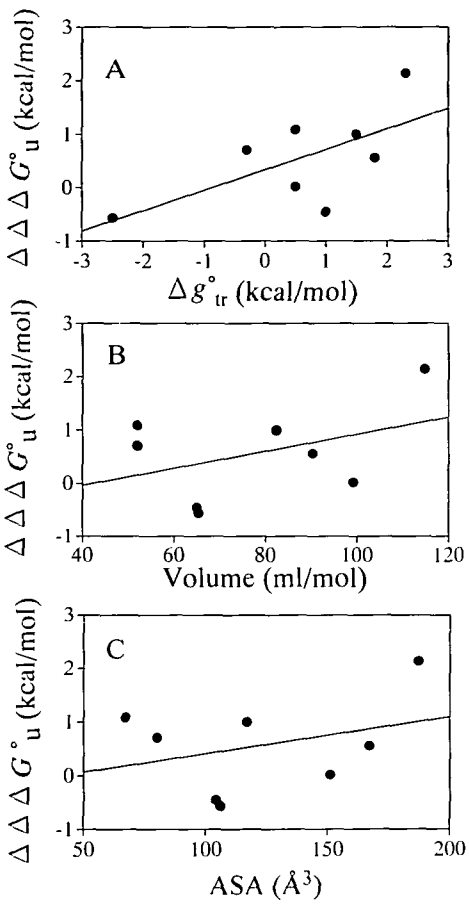

Fig. 5. **Plots of $\Delta\Delta\Delta G^{\circ}_{u}$ against the hydrophobicity (A), volume (B), and accessible surface area (C) of introduced amino acid side chains at site 121.** The $\Delta\Delta\Delta G^{\circ}_{u}$ values were calculated with Eq. 6. The Δg°_{tr}, molar volume, and ASA values were taken from Nozaki and Tanford (*42*), Zamyatnin (*43*), and Miller *et al.* (*44*), respectively. Solid lines indicate the results of the least-squares fittings: the correlation coefficients were 0.643, 0.441, and 0.353 for panels A, B, and C, respectively.

the K_m value of G67V/G121V seems to be considerably larger than with those of the corresponding single mutants, G67V and G121V (Table II). The K_m value of G67V/G121A recovers to the level of the wild-type DHFR, although the corresponding single mutants, G67V and G121A, have a larger K_m value. These results suggest that the long-range interaction might slightly influence the substrate-enzyme interaction.

The changes of k_{cat} value are not so easily rationalized, since the rate-limiting step may change in the mutants. It is known that the rate-limiting step of the wild-type DHFR changes from the product-releasing step at neutral pH to the hydride transfer step at pHs above 8.4 (*24*), and that the mutations alter the rate-limiting step to the hydride transfer step even at neutral pH (*36-39*). From the deuterium isotope effect (*29*) on k_{cat} with NADPD ([4′(*R*)-^{2}H]NADPH) instead of NADPH, we also found that the rate-limiting step of some mutant DHFRs at site 67 (G67C and G67D) changes to the hydride transfer step at neutral pH (*7*). Although such tests were not done in the present study, we may expect some modification of the rate-limiting step for the double mutants. If we examine the effects of amino acid residues at site 121, k_{cat} decreases in the order of Ala > Leu > His > Cys > Ser > Tyr > Val > Asp for double mutants but in the order of Ala > Cys > Ser > His > Tyr > Val = Leu > Asp for single mutants. These two orders are consistent with each other except for leucine and histidine. This predicts that k_{cat} is dominantly determined by the mutation at site 121.

The contribution of a mutation to the enzyme function can be quantitatively evaluated from the change in transition-state stabilization energy, $\Delta\Delta G^{*}$ (*40*),

$$\Delta\Delta G^{*} = -RT \ln \{(k_{cat}/K_m)_{mutant}/(k_{cat}/K_m)_{wild}\} \quad (7)$$

$\Delta\Delta G^{*}$ represents the difference in free energy changes of wild-type and mutant enzymes to reach the transition-state complex (E•S*) from the free enzyme and substrate (E + S). By analogy to Scheme I, contributions of the long-range interaction to $\Delta\Delta G^{*}$ can be calculated as follows.

$$\begin{aligned}\Delta\Delta\Delta G^{*} &= \Delta\Delta G^{*}_{V67,G121\text{-}X} - \Delta\Delta G^{*}_{G67,G121\text{-}X} \\ &= [RT \ln \{(k_{cat}/K_m)_{G121X}/(k_{cat}/K_m)_{wild}\}] \\ &\quad - [RT \ln \{(k_{cat}/K_m)_{G67V/G121X} \\ &\quad /(k_{cat}/K_m)_{G67V}\}] \end{aligned} \quad (8)$$

The obtained values of $\Delta\Delta G^{*}_{V67,G121\text{-}X}$, $\Delta\Delta G^{*}_{G67,G121\text{-}X}$, and $\Delta\Delta\Delta G^{*}$ are listed in Table IV. Evidently, the $\Delta\Delta\Delta G^{*}$ values are zero or negligibly small for the five mutations to serine, aspartic acid, valine, histidine, and tyrosine, suggesting that the effects of these mutations on the transition-state stabilization energy of DHFR are additive. On the other hand, the three mutations to alanine, cysteine, and leucine showed considerable positive or negative values of $\Delta\Delta\Delta G^{*}$, indicating the contribution of interaction between the two mutation sites to the enzyme function. As reviewed by Wells (*41*), the effects of double mutation on the transition-state stabilization energy are essentially additive in many proteins, with two exceptions: when the two residues are in a close contact; and when the mutation at either site changes the mechanism or rate-limiting step of the enzyme reaction. In the present case, the distance between sites 67 and 121 is more than 27 Å, and the nonadditive effects could thus be attributed mainly to the modification of the rate-limiting step. In that the rate-limiting step of DHFR is affected by the single mutations at site 67, the nonadditive effects of these three double mutants are not surprising.

No definite correlation was found between $\Delta\Delta\Delta G^{\circ}_{u}$ and $\Delta\Delta\Delta G^{*}$. This means that the nonadditive mutation in the structural stability is not always nonadditive in the enzyme function. For example, G67V/G121Y has greatly enhanced stability compared with the single mutants, but its function is additive (Tables III and IV). This result suggests that the stability and function of this enzyme are not determined by the same strategy for amino acid substitution in evolution but by more complicated regulation. It is highly possible that the long-range interaction is caused by structural perturbations or the overall dynamics.

As demonstrated in this study, double mutation in the flexible loops, Gly67 and Gly121, can influence additively or nonadditively the structure, stability, and function of DHFR. The nonadditivity effects confirm the existence of the long-range interactions between two sites which are separated by 27.7 Å. This means that a small alteration in local atomic packing due to the amino acid substitution is

TABLE IV. $\Delta\Delta G^{*}_{C121-X}$ and $\Delta\Delta\Delta G^{*}$ values calculated from the kinetic parameters in Table II.[a]

Residue at site 121	$\Delta\Delta G^{*}_{C121-X}$ (kcal/mol)		$\Delta\Delta\Delta G^{*}$ (kcal/mol)
	Glycine-67	Valine-67	
Ser	1.1	1.4	0.3
Ala	1.0	0.3	−0.7
Cys	0.7	1.1	0.5
Asp	2.2	2.2	0.0
Val	1.9	1.9	0.0
His	1.2	0.9	−0.3
Leu	2.2	1.0	−1.3
Tyr	1.3	1.5	0.2

[a]The $\Delta\Delta G^{*}_{C121-X}$ and $\Delta\Delta\Delta G^{*}$ values were calculated with Eqs. 7 and 8, respectively.

dramatically magnified over almost the whole molecule, *via* "stepwise atomic reconstruction or cooperative structural perturbations." Such a long-range interaction does not necessarily contribute to the stability and function to the same extent. These findings provide evidence that the flexible loops play important roles in protein dynamics by determining the stability and function. More systematic mutation studies are required in order to find an algorism to characterize and design the long-range interactions in protein engineering.

We wish to thank Dr. M. Iwakura of the National Institute for Advanced Interdisciplinary Research for the gifts of plasmid pTP64-1 and *E. coli* strain D3-157, and Prof. K. Yoshikawa of the Faculty of Human Informatics of Nagoya University for the use of the J-720W spectropolarimeter. We also thank the Nagoya University Computer Center for the use of the SALS program.

REFERENCES

1. Bolin, J.T., Filman, D.J., Matthews, D.A., Hamlin, R.C., and Kraut, J. (1982) Crystal structures of *Escherichia coli* and *Lactobacillus casei* dihydrofolate reductase refined at 1.7 Å resolution. *J. Biol. Chem.* **257**, 13650-13662
2. Bystroff, C., Oatley, S.J., and Kraut, J. (1990) Crystal structures of *Escherichia coli* dihydrofolate reductase: The $NADP^+$ holoenzyme and the folate·$NADP^+$ ternary complex. Substrate binding and a model for the transition state. *Biochemistry* **29**, 3263-3277
3. Bystroff, C. and Kraut, J. (1991) Crystal structure of unliganded *Escherichia coli* dihydrofolate reductase: Ligand-induced conformational changes and cooperativity in binding. *Biochemistry* **30**, 2227-2239
4. Epstein, D.M., Benkovic, S.J., and Wright, P.E. (1995) Dynamics of the dihydrofolate reductase-folate complex: catalytic sites and regions known to undergo conformational change exhibit diverse dynamical features. *Biochemistry* **34**, 11037-11048
5. Gekko, K., Yamagami, K., Kunori, Y., Ichihara, S., Kodama, M., and Iwakura, M. (1993) Effects of point mutations in a flexible loop on the stability and enzymatic function of *Escherichia coli* dihydrofolate reductase. *J. Biochem.* **113**, 74-80
6. Gekko, K., Kunori, Y., Takeuchi, H., Ichihara, S., and Kodama, M. (1994) Point mutations at glycine-121 of *Escherichia coli* dihydrofolate reductase: Important roles of a flexible loop in the stability and function. *J. Biochem.* **116**, 34-41
7. Ohmae, E., Iriyama, K., Ichihara, S., and Gekko, K. (1996) Effects of point mutations at the flexible loop glycine-67 of *Escherichia coli* dihydrofolate reductase on its stability and function. *J. Biochem.* **119**, 703-710
8. Shortle, D. and Meeker, A.K. (1986) Mutant forms of staphylococcal nuclease with altered patterns of guanidine hydrochloride and urea denaturation. *Proteins: Struct. Funct. Genet.* **1**, 81-89
9. Hecht, M.H., Sturtevant, J.M., and Sauer, R.T. (1986) Stabilization of lambda repressor against thermal denaturation by site-directed Gly→Ala changes in alpha-helix 3. *Proteins: Struct. Funct. Genet.* **1**, 43-46
10. Hurle, M.R., Tweedy, N.B., and Matthews, C.R. (1986) Synergism in folding of a double mutant of the alpha subunit of tryptophan synthase. *Biochemistry* **25**, 6356-6360
11. Wetzel, R., Perry, L.J., Baase, W.A., and Becktel, W.J. (1988) Disulfide bonds and thermal stability in T4 lysozyme. *Proc. Natl. Acad. Sci. USA* **85**, 401-405
12. Sandberg, W.S. and Terwilliger, T.C. (1993) Engineering multiple properties of a protein by combinatorial mutagenesis. *Proc. Natl. Acad. Sci. USA* **90**, 8367-8371
13. Akasako, A., Haruki, M., Oobatake, M., and Kanaya, S. (1995) High resistance of *Escherichia coli* ribonuclease HI variant with quintuple thermostabilizing mutations to thermal denaturation, acid denaturation, and proteolytic degradation. *Biochemistry* **34**, 8115-8122
14. Goldman, E.R., Dall'Acqua, W., Braden, B.C., and Mariuzza, R.A. (1997) Analysis of binding interactions in an idiotope-anti-idiotope protein-protein complex by double mutant cycles. *Biochemistry* **36**, 49-56
15. Serrano, L., Horovitz, A., Avron, B., Bycroft, M., and Fersht, A.R. (1990) Estimating the contribution of engineered surface electrostatic interactions to protein stability by using double-mutant cycles. *Biochemistry* **29**, 9343-9352
16. Green, S.M. and Shortle, D. (1993) Patterns of nonadditivity between pairs of stability mutations in staphylococcal nuclease. *Biochemistry* **32**, 10131-10139
17. Blaber, M., Baase, W.A., Gassner, N., and Matthews, B.W. (1995) Alanine scanning mutagenesis of the alpha-helix 115-123 of phage T4 lysozyme: Effects on structure, stability and the binding of solvent. *J. Mol. Biol.* **246**, 317-330
18. Perry, K.M., Onuffer, J.J., Gittelman, M.S., Barmat, L., and Matthews, C.R. (1989) Long-range electrostatic interactions can influence the folding, stability, and cooperativity of dihydrofolate reductase. *Biochemistry* **28**, 7961-7968
19. Texter, F.L., Spencer, D.B., Rosenstein, R., and Matthews, C.R. (1992) Intramolecular catalysis of a proline isomerization reaction in the folding of dihydrofolate reductase. *Biochemistry* **31**, 5687-5691
20. Dion, A., Linn, C.E., Bradrick, T.D., Georghiou, S., and Howell, E.E. (1993) How do mutations at phenylalanine-153 and isoleucine-155 partially suppress the effects of the aspartate-27→serine mutation in *Escherichia coli* dihydrofolate reductase? *Biochemistry* **32**, 3479-3487
21. Iwakura, M. and Tanaka, T. (1992) Dihydrofolate reductase gene as a versatile expression marker. *J. Biochem.* **111**, 31-36
22. Sanger, F., Nicklen, S., and Coulson, A.R. (1977) DNA sequencing with chain-terminating inhibitors. *Proc. Natl. Acad. Sci. USA* **74**, 5463-5467
23. Singer, S., Ferone, R., Walton, L., and Elwell, L. (1985) Isolation of a dihydrofolate reductase-deficient mutant of *Escherichia coli*. *J. Bacteriol.* **164**, 470-472
24. Fierke, C.A., Johnson, K.A., and Benkovic, S.J. (1987) Construction and evaluation of the kinetic scheme associated with dihydrofolate reductase from *Escherichia coli*. *Biochemistry* **26**, 4085-4092
25. Nakagawa, T. and Oyanagi, Y. (1980) Program system SALS for nonlinear least-squares fitting in experimental sciences in *Recent Developments in Statistical Inference and Data Analysis* (Matsushita, K., ed.) pp. 221-225, North Holland Publishing Company, Amsterdam
26. Pace, C.N. (1985) Determination and analysis of urea and guanidine hydrochloride denaturation curves in *Methods in Enzymology* (Hirs, C.H.W. and Timasheff, S.N., eds.) Vol. 131, pp. 267-280, Academic Press, New York
27. Williams, J.W., Morrison, J.F., and Duggleby, R.G. (1979) Methotrexate, a high-affinity pseudosubstrate of dihydrofolate reductase. *Biochemistry* **18**, 2567-2573
28. Penner, M.H. and Frieden, C. (1985) Substrate-induced hysteresis in the activity of *Escherichia coli* dihydrofolate reductase. *J. Biol. Chem.* **260**, 5366-5369

29. Stone, S.R. and Morrison, J.F. (1982) Kinetic mechanism of the reaction catalyzed by dihydrofolate reductase from *Escherichia coli*. *Biochemistry* **21**, 3757-3765
30. Kuwajima, K., Garvey, E.P., Finn, B.E., Matthews, C.R., and Sugai, S. (1991) Transient intermediates in the folding of dihydrofolate reductase as detected by far-ultraviolet circular dichroism spectroscopy. *Biochemistry* **30**, 7693-7703
31. Touchette, N.A., Perry, K.M., and Matthews, C.R. (1986) Folding of dihydrofolate reductase from *Escherichia coli*. *Biochemistry* **25**, 5445-5452
32. Perry, K.M., Onuffer, J.J., Touchette, N.A., Herndon, C.S., Gittelman, M.S., Matthews, C.R., Chen, J.T., Mayer, R.J., Taira, K., Benkovic, S.J., Howell, E.E., and Kraut, J. (1987) Effect for single amino acid replacements on the folding and stability of dihydrofolate reductase from *Escherichia coli*. *Biochemistry* **26**, 2674-2682
33. Garvey, E.P. and Matthews, C.R. (1989) Effects of multiple replacements at a single position on the folding and stability of dihydrofolate reductase from *Escherichia coli*. *Biochemistry* **28**, 2083-2093
34. Jennings, P.A., Finn, B.E., Jones, B.E., and Matthews, C.R. (1993) A reexamination of the folding mechanism of dihydrofolate reductase from *Escherichia coli*: Verification and refinement of a four-channel model. *Biochemistry* **32**, 3783-3789
35. Iwakura, M., Jones, B.E., Falzone, C.J., and Matthews, C.R. (1993) Collapse of parallel folding channels in dihydrofolate reductase from *Escherichia coli* by site-directed mutagenesis. *Biochemistry* **32**, 13566-13574
36. David, C.L., Howell, E.E., Farnum, M.F., Villafranca, J.E., Oatley, S.J., and Kraut, J. (1992) Structure and function of alternative proton-relay mutants of dihydrofolate reductase. *Biochemistry* **31**, 9813-9822
37. Chen, J.-T., Taira, K., Tu, C.-P.D., and Benkovic, S.J. (1987) Probing the functional role of phenylalanine-31 of *Escherichia coli* dihydrofolate reductase by site-directed mutagenesis. *Biochemistry* **26**, 4093-4100
38. Howell, E.E., Warren, M.S., Booth, C.L., Villafranca, J.E., and Kraut, J. (1987) Construction of an altered proton donation mechanism in *Escherichia coli* dihydrofolate reductase. *Biochemistry* **26**, 8591-8598
39. Warren, M.S., Brown, K.A., Farnum, M.F., Howell, E.E., and Kraut, J. (1991) Investigation of the functional role of tryptophan-22 in *Escherichia coli* dihydrofolate reductase by site-directed mutagenesis. *Biochemistry* **30**, 11092-11103
40. Wilkinson, A.J., Fersht, A.R., Blow, D.M., and Winter, G. (1983) Site-directed mutagenesis as a probe of enzyme structure and catalysis: tyrosyl-tRNA synthetase cysteine-35 to glycine-35 mutation. *Biochemistry* **22**, 3581-3586
41. Wells, J.A. (1990) Additivity of mutational effects in proteins. *Biochemistry* **29**, 8509-8517
42. Nozaki, Y. and Tanford, C. (1971) The solubility of amino acids and two glycine peptides in aqueous ethanol and dioxane solutions. *J. Biol. Chem.* **246**, 2211-2217
43. Zamyatnin, A.A. (1984) Amino acid, peptide, and protein volume in solution. *Annu. Rev. Biophys. Bioeng.* **13**, 145-165
44. Miller, S., Janin, J., Lesk, A.M., and Chothia, C. (1987) Interior and surface of monomeric proteins. *J. Mol. Biol.* **196**, 641-656